Research Article | Vol. 29, No. 24 / 22 Nov 2021 / Optics Express 39227

Optics EXPRESS

In-plane directionality control of strongly localized resonant modes of light in disordered arrays of dielectric scatterers

A. K. M. NAZIUL HAQUE,[1,2,3] TASHFIQ AHMED,[1,3] AND MD ZUNAID BATEN[1,*]

[1] *Department of Electrical and Electronic Engineering, Bangladesh University of Engineering and Technology, Dhaka, Bangladesh*
[2] *Department of Computer Science and Engineering, Brac University, Dhaka, Bangladesh*
[3] *These authors contributed equally to this work*
[*] *mdzunaid@eee.buet.ac.bd*

Abstract: In this work we propose and analyze techniques of in-plane directionality control of strongly localized resonant modes of light in random arrays of dielectric scatterers. Based on reported diameters and areal densities of epitaxially grown self-organized nanowires, two-dimensional (2D) arrays of dielectric scatterers have been analyzed where randomness is gradually increased along a preferred direction of directionality enhancement. In view of the multiple-scattering mediated wave dynamics and directionality enhancement of light in such arrays, a more conveniently realizable, practical structure is proposed where a 2D periodic array is juxtaposed with a uniform, random scattering medium. Far- and near-field emission characteristics of such arrays show that in spite of the utter lack of periodicity in the disordered regime of the structure, directionality of the high-Q resonant modes is modified such that on average more than 70% of the output power is emitted along the pre-defined direction of preference. Such directionality enhancement and strong localization are nonexistent when the 2D periodic array is replaced with a one-dimensional Bragg reflector, thereby confirming the governing role of in-plane multiple scattering in the process. The techniques presented herein offer novel means of realizing not only directionality tunable edge-emitting random lasers but also numerous other disordered media based photonic structures and systems with higher degrees of control and tunability.

© 2021 Optical Society of America under the terms of the OSA Open Access Publishing Agreement

1. Introduction

Disorder photonics is an exotic area of photonic research which offers the prospect of tailoring the behavior of light in random systems rather than in conventional periodic ones [1,2]. Intensive research in this area over the last few decades has encouraged exploitation of the spatial localization or spectral broadening of light in disordered media for practical applications ranging from lasing [3–5] to energy harvesting [6,7], imaging [8,9] and sensing [10,11]. Notwithstanding such progress, one of the longstanding challenges associated with the field of disordered photonics is the controllability of the directionality of light in a random medium. This challenge is particularly relevant to the development of random lasers, which are mirror-less systems relying on random scattering of light for photon entrapment in a gain medium. Whereas directionality of conventional edge-emitting lasers or vertical cavity surface emitting lasers can be controlled by designing the cavity facet or surface aperture, far-field radiation patterns of random lasers are rather unpredictable because of the multiple scattering mediated wave dynamics of light in the underlying disordered medium.

Directionality control of light in disordered media has continued to be an active area of research in the context of random lasers. In one of the early works comprising passive scatterers in a homogeneous active dye solution, it has been shown that lasing output is preferentially obtained

#443103 https://doi.org/10.1364/OE.443103
Journal © 2021 Received 13 Sep 2021; revised 27 Oct 2021; accepted 30 Oct 2021; published 9 Nov 2021

along the direction in which the gain medium is most extended [12]. Directionality control has also been attained from a random system of organic-inorganic sol-gel film, sandwiched between two dielectric Bragg reflectors (DBRs) [13]. Modification of the spatial pump distribution by wavefront shaping [14] and tuning of pump energy [15] have also been proposed as techniques of directionality control of random lasers. In a more recent work relevant to this research, a semiconductor gain medium consisting of random nanopores was placed within two metallic waveguides to obtain out-of-plane, directional lasing emission [16]. Directionality control has also been reported employing Anderson localizing optical fiber fabricated by polymer and glass (g-ALOF), where co-existence of transverse-random localization and Fabry-Perot resonance at the air-fiber interface results in a directional output [17].

In spite of the mentioned significant achievements, a scenario that has remained unattended in the context of directionality control of light in disordered systems is the case of in-plane directionality control of light emanating from a two-dimensional array of dielectric scatterers. Control over output directionality in such systems is highly relevant to the practical realization of edge-emitting lasers based on self-organized nanowire arrays. These nanowire arrays- usually grown by techniques like molecular beam epitaxy (MBE) [18,19], metal-organic chemical vapor deposition (MOCVD) [20], atomic-layer deposition (ALD) [21]- constitute among themselves uniform random media which are highly suitable for exploring phenomena related to multiple-scattering mediated localization of light. Moreover, the scope of embedding semiconductor heterostructures in such random arrays of nanowires offers the prospect of realizing lasers with tunable emission characteristics. In fact, III-nitride variants of such nanowire arrays have already been utilized for realizing edge-emitting lasers ranging from visible to near-infrared (NIR) regime of the spectrum [22], and more recently a monolithic photonic integrated circuit has also been demonstrated based on such arrays [23]. The ability to control in-plane directionality of light in such random arrays would therefore remarkably enhance the prospect of realizing future photonic and optoelectronic devices and systems with a high degree of design latitude.

In the present study, we propose and analyze a technique of controlling in-plane directionality of the resonant mode of light localized in a random array of dielectric scatterers. In accordance with reported dimensionalities of self-organized GaN nanowires grown by MBE systems, both correlated and uniform random arrays of dielectric scatterers have been systematically generated in this work. Finite difference time domain (FDTD) technique based numerical analysis of the correlated random arrays show that output directionality can be significantly enhanced by gradually introducing randomness along the direction of preference. Based on results of the correlated system and in view of feasibility of practical implementation, a structure is proposed where the uniform random array is juxtaposed with a periodic array such that localized mode of the disordered medium is emitted along the preferred half-plane of the overall structure. Statistical analysis of the far- and near-field emission characteristics show that high-Q resonant modes, having quality factors ranging from $10^4 - 10^6$ are localized in the disordered region of these arrays, and on average about 70% (with the maximum value approaching 95%) of the output power of these modes is emitted along the predefined direction of preference. In conclusion, techniques of practical realization of the proposed structure have also been mentioned in the context of directionality enhancement of self-organized nanowire array based photonic devices and systems.

2. Directionality of correlated random arrays

In previous studies on strong-localization of light in self-organized GaN nanowire arrays, it has been shown that depending on diameter and areal density of nanowires, transverse-magnetic (TM) modes spanning over near-UV to visible regime of the spectra are localized within the arrays with quality (Q) factors ranging from $10^4 - 10^6$ [19,24]. The attainment of such large Q-factors in a random array of scatterers is intricately related to the phenomenon of Anderson localization of light in random media. This phenomenon was originally proposed to explain the behavior of electron transport in a disordered solid-state system, where interference between multiple scattered electron waves results in a complete halt of electron transport [25–27]. The optical analogy of Anderson localization has been consistently observed in photonic systems comprising disordered media like random arrays of GaN and ZnO nanocolumns [18,20], random fractal array of silicon nanowires [28], core-shell TiO_2 nanowires [21], silicon-nitride photonic crystal waveguides [29], AlGaN nanowires arrays [19], self-organized GaN nanowires [18,24], selective-area grown InP nanowires [30] etc. In accordance with those studies and also in accordance with reported dimensions of MBE grown self-organized III-nitride nanowires [19,31,32], uniform random arrays of GaN nanowires have been systematically generated in this work.

Two dimensional (2D) cross-sectional view of three such arrays are shown in Figs. 1(a)-(c). The nanowire-diameter (d) and fill-factor (f) of these arrays are d = 55 nm and f = 35% respectively. In spite of identical diameter and areal density, the arrays differ in terms of spatial configuration of the nanowires - just as self-organized nanowire arrays would differ in terms of spatial locations of the nanowires because of inherent randomness of the growth process [33]. Near- and far-field emission characteristics of these arrays have been evaluated based on finite difference time domain (FDTD) analysis technique employing the open source software package MEEP [34]. Throughout this study, a Gaussian pulse source has been positioned at the center of the array. Resonant modes of the photonic structure have been computed by decomposition of electric and magnetic field components of the electromagnetic (EM) wave using filter diagonalization method [35]. In order to model an open system, a phase matched layer (PML) having thickness greater than the source-wavelength has been considered around the computational region, which ensures that non-localized EM wave is not reflected back into the array. Based on this simulation framework, resonant wavelength (λ_r) and quality factor (Q) of the most strongly localized modes of the arrays shown in Figs. 1(a)-(c) are calculated and the corresponding far-field directionality profiles are obtained. The far-field patterns of Fig. 1(d) show that in spite of identical diameter and areal density of the scatterers, in-plane directionality of these localized modes remains entirely random for all practical purposes. Such randomness arises from the underlying multiple scattering dynamics of light in the intrinsically disordered medium.

In spite of the utter lack of periodicity in such arrays and the consequent random scattering events, it has been shown both theoretically and experimentally that resonant wavelengths of strongly localized modes of a disordered medium can be red-shifted by increasing diameters of the scatterers, provided that the fill-factor is within the desired range to enable strong-localization of light [19,24]. To understand whether similar tunability of directionality characteristics can be obtained by varying diameter and fill factor, correlated random arrays are systematically generated and analyzed in this work. In order to understand the effect of diameter variation, correlated arrays having nanowire diameter of 50 nm, 55 nm and 60 nm are considered. In these arrays (shown in Figs. 1(e)-(g)), spatial location of the nanowires have been kept identical so that the change of directionality characteristics can be attributed to the change of diameter variation alone. Far-field directionality profiles of the most strongly confined TM modes of these arrays are shown in Fig. 1(h). As can be observed, for 5 nm variation of the diameter, the far-field pattern changes substantially and the trend is entirely random. In fact, having analyzed diameter variation with a smaller margin of 1 nm, it is observed that the directionality profile changes randomly even when spatial positions of the nanowires is kept unchanged. These results suggest that directionality characteristics of uniform random dielectric scattering media representing self-organized nanowires cannot be tuned by controlling diameters of the scatterers.

In order to assess the effect of areal density i.e. fill factor variation, correlated random arrays of nanowires having 50 nm diameter are generated by randomly introducing new nanowires in the array while keeping locations of the existing nanowires intact. The resultant arrays, having fill factors of 30%, 35% and 40% respectively, are shown in Figs. 1(i)–1(k). Far-field directionality

Optics EXPRESS

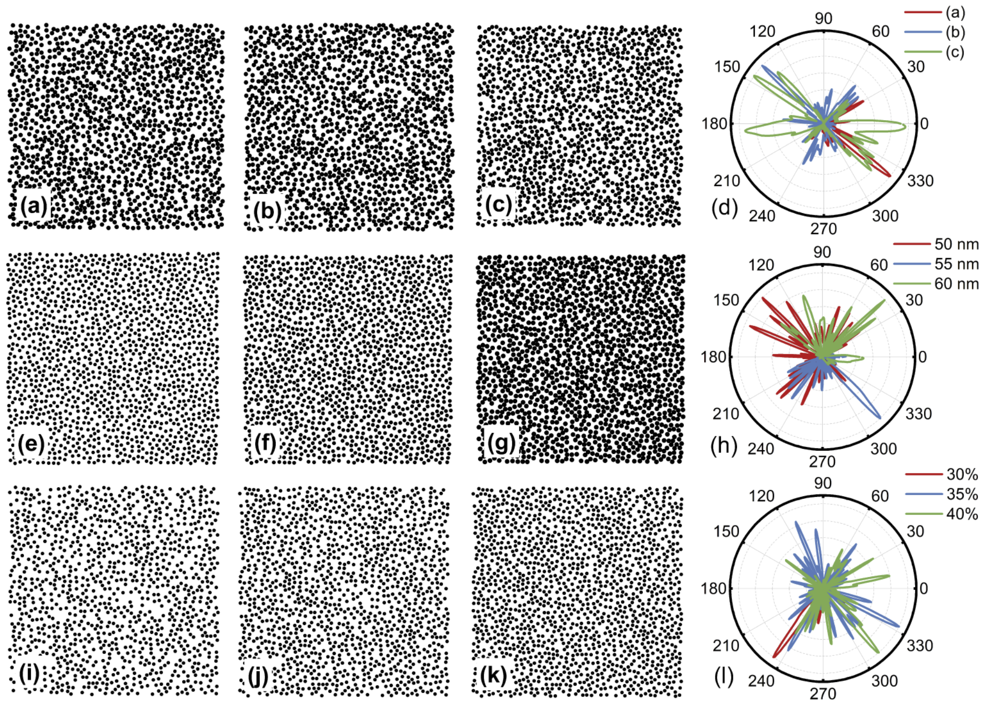

Fig. 1. (a)-(c) Three uniform random arrays having nanowire diameter, d = 55 nm and fill factor, f = 35%, and (d) far-field radiation patterns of the most strongly localized modes of these arrays located at 285 nm, 284 nm and 279 nm respectively. Correlated random arrays with fixed positions of the nanowires having diameters of (e) d = 50 nm, (f) d = 55 nm, (g) d = 60 nm respectively, and (h) far-field radiation patterns of the most strongly localized modes of these arrays having resonant wavelengths of 280 nm, 282 nm and 294 nm respectively. Correlated random arrays with fixed diameter of 50 nm, and fill-factors of (i) f = 30%, (j) f = 35%, (k) f = 40% respectively, while nanowires are gradually added in empty locations of the array; (l) the far-field directionality profiles of the most strongly localized modes in these arrays are located at 286 nm, 296 nm and 290 nm respectively.

profiles of these arrays (shown in Fig. 1(l)) indicate that similar to the case of diameter variation, directionality remains random for gradual variation of fill factor in the arrays, even when spatial correlation between nanowire positions of each array is maintained. These results suggest that though resonant wavelength, as well as transmission gap of random arrays can be tuned by varying diameter and fill factor of the scatterers [24,36], a different approach needs to be adopted to control directionality of the resonant modes of such disordered media. To this end we explore and analyze novel photonic structures in the subsequent sections to attain random scattering mediated strong localization of light while ensuring controllability of their directionality characteristics.

3. Formation and analysis of structures for directionality control

In our previous study on directionality control of whispering gallery resonant modes of rotationally symmetric nanowire arrays [37], it has been shown that omnidirectional far-field pattern can be made unidirectional by controllably varying nanowire spacing along the preferred axis of directionality. To understand whether such uniaxial variation of nanowire spacing can enhance directionality of a disordered array of nanowires, we adopt the GaN nanowire array shown in Fig. 2(a). This arrangement, which is referred to as ’Structure 1’ or ’uniaxial gradual random’ structure hereon, is generated based on the periodic template shown in Fig. 2(b).

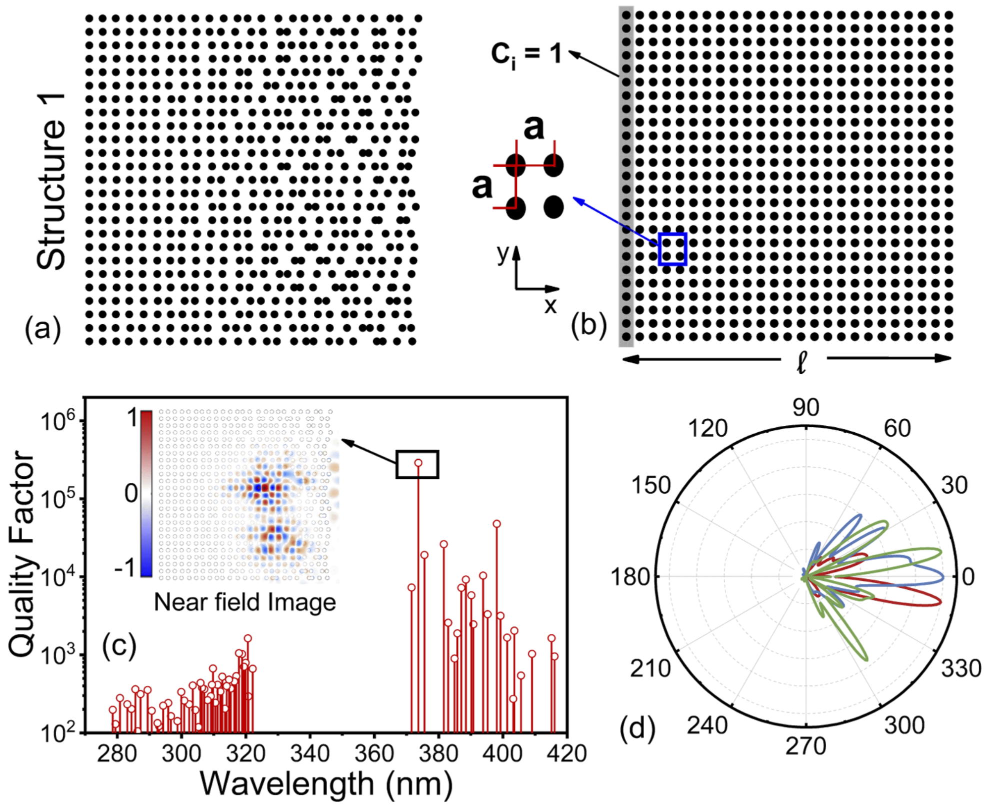

Fig. 2. (a) Uniaxial gradual random structure, which has been generated from the two-dimensional (2D) periodic structure shown in (b); (c) quality factor (Q_f) plotted as a function of wavelength for Structure 1 (inset shows near-field image of the mode having the highest Q-factor); (d) far-field directionality profiles of the most strongly-localized modes, obtained for three different spatial configurations of Structure 1

The cross-sectional area of this periodic template is $l \times l$, where m number of equally spaced nanowires are positioned a distance apart along each row and column. The center position of a nanowire in this array is described by (x, y). Then the center position of the corresponding nanowire of a uniaxial gradual random structure (Fig. 2(a)) is defined as $(x + \delta x, y)$, where

$$\delta x = \frac{ra(C_i - 1)}{2(m - 1)} \tag{1}$$

Here r is a uniformly distributed random number in the range [-1, 1] and C_i $(= 1, 2, 3, \ldots, m)$ is the column index of that nanowire in the periodic array of Fig. 2(b). According to Eq. (1), the degree of randomness in Structure 1 uniaxially increases from left to right end of the array. By considering $l = 3$ μm, $a = 120$ nm, $d = 70$ nm and $f = 27\%$, multiple configurations of uniaxially random arrays have been generated and analyzed. As has been shown in previous studies, the $3\mu m \times 3\mu m$ array size is significantly larger than the light localization area in ntiride nanowire based random arrays [36,37]. This is considered to be one of the preconditions for attaining localization of light in such disordered systems. To understand whether these arrays represent weakly or strongly disordered systems, disorder strength (ζ) is calculated as per the following relation [38]:

$$\zeta = 1 - \frac{1}{N-1}\sum_{i=1}^{N}\left(\frac{A_i-\mu_A}{\sigma_A}\right)\left(\frac{B_i-\mu_B}{\sigma_B}\right) \tag{2}$$

Here μ_A (σ_A) and μ_B (σ_B) are mean (standard deviation) of matrix A and B respectively. Matrix A (B) represents an one-dimensional (1D) matrix, which is created by cascading consecutive rows of the two-dimensional refractive index profile of the periodic (disordered) array. The two-dimensional refractive index profile is created by discretizing the two-dimensional nanowire array into N number of grid points along both x- and y-axis of the array. The distance between each grid point is kept such that it is much smaller than the diameter of the nanowires considered in this work. As each point of the grid contains the refractive index of that specific location of the array, a $N \times N$ matrix is created which contains refractive index information of the entire structure. Based on such discretization and transformation, the 1D matrices A and B shown in Eq. (2) have been created. It is to be noted that the periodic structure shown in Fig. 2(b) is taken as a common reference to compute disorder strength of all the arrays in this work, i.e. matrix A in Eq. (2) contains the refractive indices of each point of the fully periodic system shown in Fig. 2(b). On the other hand, array B contains the refractive indices of each point of any other array considered in this study. Correlation between A and B as per Eq. (2) provides the disorder strength of the structure under consideration.

For multiple random configurations of Structure 1, the calculated disorder strength lies within a range of 28-33%. In our previous study it has been shown that light remains strongly localized in GaN nanowire arrays of $\zeta \geq 30\%$ [37]. Therefore it is expected that the uniaxial gradual random array of Structure 1 would result in strong localization of light. This is confirmed by the calculated high-Q resonant modes of Structure 1. As can be observed from Fig. 2(c), Q-factor of the most strongly confined mode in this array is about 3×10^5, which is similar to the Q-factors obtained for strongly-localized resonant modes in III-nitride nanowire arrays [19,24]. As discussed earlier, the emergence of such high-Q resonant modes is attributed to the multiple-scattering mediated Anderson localization phenomena in highly disordered media. The near-field image of the most strongly confined mode (shown as an inset of Fig. 2(c)) also confirms the localization of light in the disordered portion of the array. Far-field radiation pattern (shown in Fig. 2(d)) of this strongly confined mode clearly exhibits nearly-unidirectional emission characteristics along the direction of high degree of disorder, i.e. along the right-half side of the array. To ascertain that such directionality along the direction of high degree of disorder is not coincidental, 30 different spatial configurations of Structure 1 have been calculated and analyzed. Far-field radiation patterns of three such arrays are shown in Fig. 2(d). It is quite obvious that contrary to the randomness observed for the cases illustrated in Fig. 1, light output remains nearly unidirectional for different spatial configurations of Structure 1.

A close examination of Structure 1 suggests that left-half side of this array contains a rather small degree of randomness and it very much resembles a periodic structure. In fact disorder strength of left-half side (within the range $-\frac{l}{2} \leq x \leq 0$) of the array is calculated to be 13.48%, whereas for the right-half side $\zeta = 48.5\%$. This suggests that localization of light is primarily governed by the disorder extending over right-half side of the array. Based on this observation, a second structure denoted as Structure 2 (shown in Fig. 3(a)) is proposed and analyzed. In this new arrangement, the left-half side consists of a periodic array having nanowire spacing of $a = 120$ nm, and the right-hand side comprises a disordered system having uniform randomness along x-axis of the structure. In accordance with the definition of Eq. (1), such an half-periodic, half-uniaxially random structure can be mathematically expressed using the following relation:

$$\delta x = \begin{cases} 0 & ; 1 \leq C_i \leq \lceil \frac{m}{2} \rceil \\ \frac{ra}{2} & ; otherwise \end{cases} \tag{3}$$

Optics EXPRESS

The far and near-field radiation patterns of Structure 2 are shown in Figs. 3(b)-(c). As can be observed, directionality and localization characteristics similar to those of Structure 1 are obtained for Structure 2, i.e. the most strongly localized mode is emitted along the direction of high degree of disorder. Such characteristics are obtained irrespective of spatial configurations of the array. Far-field radiation patterns of three representative arrays of Structure 2 are shown in Fig. 3(b). As can be observed, for all cases the main lobe of the radiation pattern is pointed towards the right-half side of the overall structure.

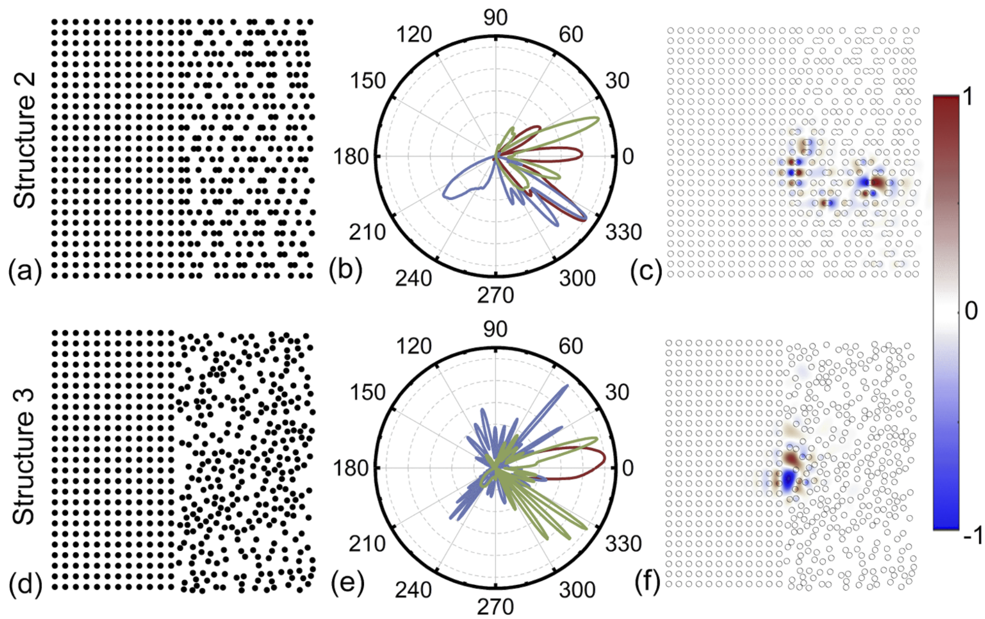

Fig. 3. (a) Representative half-periodic, half uniaxial-random array (Structure 2); (b) far-field emission patterns of the most strongly confined modes for different spatial configurations of Structure 2 and (c) near-field profile for one of the localized modes in an array of Structure 2; (d) representative half-periodic, half-uniform random array (Structure 3); (b) far-field emission patterns of the most strongly confined modes for different spatial configurations of Structure 3 and (c) near-field profile for one of the localized modes in an array of Structure 3.

The light-localization characteristics of Structure 2 suggest an important development, which is by juxtaposing a 2D periodic array with a uniaxial random one, it is possible to extract light output along a preferred direction. For different spatial configurations of Structure 2, disorder strength on the right-half side is obtained to be in the range of 62-65%. This value is significantly higher than the corresponding ζ values obtained for Structure 1. Though such disorder strengths already represent strongly disordered systems, it remains to be seen how directionality characteristics will change in the presence of a higher degree of disorder. To this end, we consider the system shown in Structure 3 (Fig. 3(d)), where the uniaxial random array of Structure 2 is replaced with a uniform random array of scatterers having identical diameter and fill factor as in Structure 1 and 2. Because this uniform random array is not derived from a periodic structure, a ζ value cannot be computed for Structure 3. It is also noteworthy that the uniform random portion of Structure 3 effectively represents self-organized GaN nanowire arrays discussed earlier. Far-field radiation patterns (shown in Fig. 3(e)) obtained for three different random configurations of Structure 3 show that similar to the cases of Structure 1 and 2, a greater fraction of light is emitted towards the right-half side of the structure. Near field distribution (shown in Fig. 3(f)) of the most strongly confined mode for one of the arrangements

Optics EXPRESS

of Structure 3 exhibits strong-localization of light with a Q-factor of 10^5. These results suggest that in-plane directionality characteristics of strongly-localized modes of a uniform random array, though is otherwise random and unpredictable, it can be appreciably controlled by introducing an appropriately designed 2D periodic array in its proximity.

4. Comparison among proposed structures

Having discussed and analyzed the three structures proposed for directionality enhancement, in this Section we compare their near- and far-field emission characteristics. To take into account statistical variation resulting from random positioning of nanowires in the arrays, 30 different spatial configurations of each of these 3 structures have been analyzed. Resonant wavelength and quality factor of the most strongly confined modes of each of these arrays are calculated and plotted in Figs. 4(a)-(b). As can be observed from Fig. 4(a), the uniaxially random arrays of Structure 1 and 2 exhibit relatively smaller variation of resonant wavelength compared to the half-periodic half-uniform random array of Structure 3. Nonetheless, the Q-factor of all the arrays lie within the range of $10^4 - 10^6$, therefore ensuring strong localization of light.

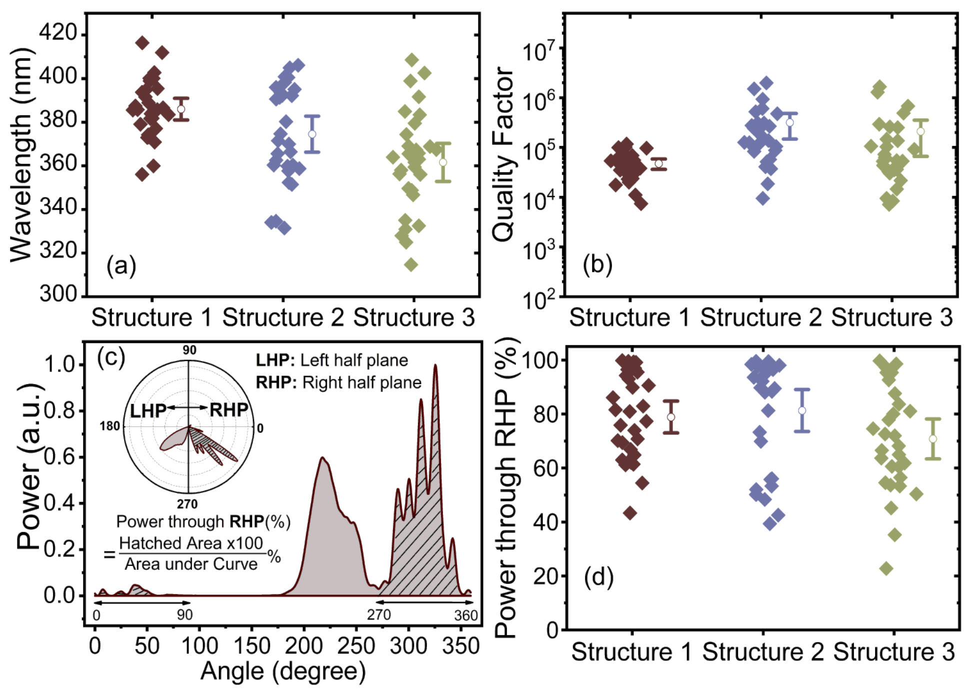

Fig. 4. Scatter plot of (a) localized wavelength and (b) quality factor obtained for different spatial configurations of Structure 1, 2 and 3; (c) power corresponding to the resonant mode plotted in arbitrary units (a.u.) as a function of angle to illustrate the calculation of percentage of power through the right-half plane (inset shows the corresponding far-field profile); (d) percentage of power through the right half plane (RHP) calculated for the spatial configurations of Structures 1, 2 and 3 considered in Figs. 4(a)-(b). The error bars appearing in Figs. 4(a), (b) and (d) indicate the mean values with 95% confidence intervals obtained for 30 arrays of each structure shown in these plots.

To have a quantitative estimate of directionality enhancement, fraction of power transmitted along a particular direction is calculated based on the approach shown in Fig. 4(c). In this approach, the region residing within polar angle (θ) of $0^\circ \leq \theta \leq 90^\circ$ and $270^\circ \leq \theta \leq 360^\circ$ is defined as the right half plane (RHP) of the array (shown as shaded region in the inset of

Fig. 4(c)). Based on this definition, the fraction of optical power transmitted along RHP of an array is calculated by computing the corresponding area under the output power plot shown in Fig. 4(c). A similar approach has been adopted to calculate the fraction of power transmitted along RHP of the most strongly confined mode of each array considered in Figs. 4(a)-(b). Such calculated values of fraction of power, denoted as P_r hereon, have been plotted and compared in Fig. 4(d) for 30 different arrays of each structure. The results of this comparison show that Structure 1 has the least amount of fluctuation of P_r among its different arrays, whereas Structure 3 exhibits the highest degree of variation. Such variation is obviously related to the high degree of disorder present in Structure 3 compared to that of Structure 1 and 2. Whereas Structure 1 and 2 have disorder strengths of 48% and 60% respectively, Structure 3 has a uniform random distribution in its disordered region. Hence there is a greater degree of variability in the random scattering process in Structure 3, and consequently the range of variation in its Q-factor and power through the RHP is higher. It is also to be noted that Q-factor and RHP power are observed to be uncorrelated for the structures, i.e. a high Q-factor does not necessarily imply a high value of power through the RHP. Notwithstanding such variations, it is noteworthy that for all three structures, the Q-factors mostly remain in the order of 10^4-10^5, and also light output is predominantly along RHP of the array. In the case of Structure 3, on average 70% of light corresponding to its most strongly localized mode is transmitted along the RHP. For uniaxial random arrays of Structure 1 and 2, this mean value is about 80%. Moreover, for a number of arrays, nearly perfect unidirectional emission characteristics (i.e. $P_r \sim 100\%$) are obtained. These results suggest that the proposed schemes offer significant control over far-field radiation patterns of disordered systems, while ensuring that strong localization of light is attained in the disordered medium.

5. Role of the periodic array on directionality control and 3D effects

Directionality and localization characteristics of light in the structures discussed so far indicate that though the multiple-scattering mediated wave dynamics on the RHP govern the resonance conditions of light in these structures, the periodic array on the left-half plane (LHP) plays an important role in defining the direction of light output. To better understand the role of the LHP, photonic bandstructure of the periodic array of Structure 2 and 3 has been calculated and plotted in Fig. 5(a). As can be observed, a photonic bandgap exists within the wavelength range of 320 nm to 400 nm. This wavelength range coincides with wavelength range over which the most strongly localized modes of all three structures are obtained. This observation may suggest that the 2D periodic or quasi-periodic arrangements residing on the LHP essentially act as back-reflectors, which reflect and enhance light output towards the right-half plane of the arrays. To understand whether similar directionality enhancement can be attained with 1D periodic structures, the LHP of Structure 3 is replaced with a distributed Bragg reflector (DBR). This new structure, denoted as Structure 4, is shown as an inset of Fig. 5(b). The DBR of Structure 4 is designed such that its stop-band (extending from 264 nm to 451 nm) overlaps with the stop-band of the 2D periodic array appearing in Structure 2 and Structure 3.

Resonant wavelength and quality factor of the most strongly confined modes of Structure 3 and 4 are compared in Figs. 5(b)-(c). Though high Q-resonant modes are attained for both these structures, the resonant modes of Structure 3 reside well within the stop band of the 2D periodic array of the LHP. On the other hand, the highest Q-factor modes of Structure 4 are scattered over a rather extended range - well beyond the stop band of the adjacent DBR. Such characteristics ultimately affect the directionality behavior of Structure 4. Comparison of the far-field profiles of Structure 3 and 4 show that whereas light is predominantly transmitted along the RHP of Structure 3, for Structure 4 there is no such preferential direction. These results suggest that the in-plane multiple scattering process inherent in the 2D periodic array plays an important role to enhance directionality characteristics of Structures 1, 2, and 3. It is likely that

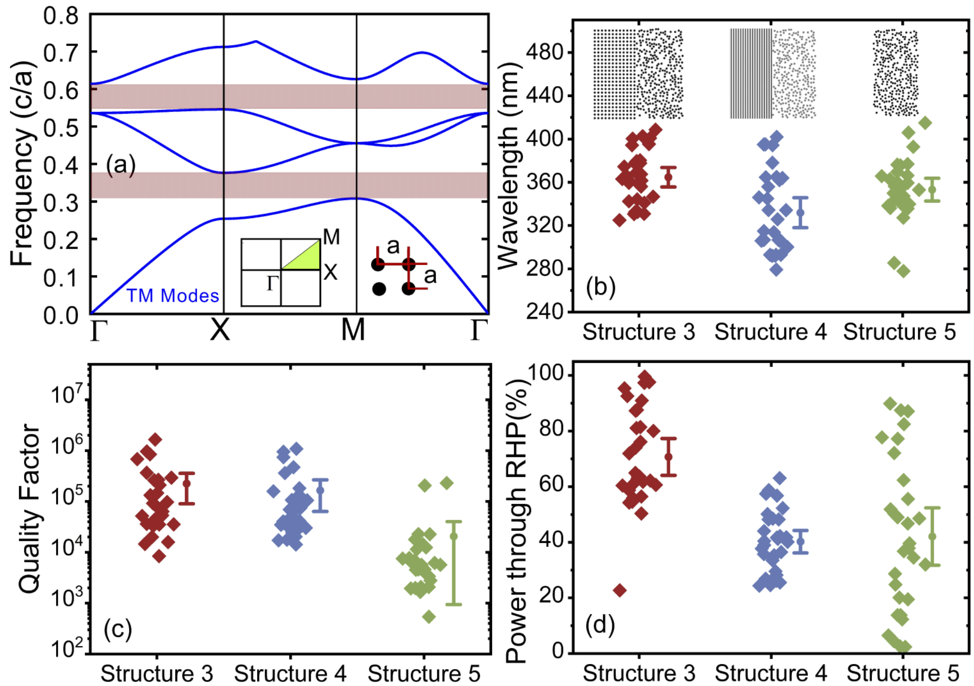

Fig. 5. (a) Photonic band structure of the 2D periodic array having lattice constant a; (b) localization wavelength, (c) quality factor and (d) percentage of power through the right-half plane (RHP) obtained for the most strongly confined modes of different spatial configurations of Structure 3, 4 and 5 (inset of Fig. 5(b) shows representative arrays of the three structures). The error bars appearing in Figs. 5(b)-(d) indicate the mean values with 95% confidence intervals obtained for 30 arrays of each structure shown in these plots.

the complex interplay between the in-plane multiple scattering in the periodic array, and the concurrent random scattering in the disordered region, enhances directionality of the overall structure along the RHP. Such a dynamics is nonexistent in Structure 4 because of the lack of in-plane multiple scattering in the one-dimensional DBR mirror. Consequently, even though the photonic bandgap is within the desired wavelength range in Structure 4, it does not exhibit enhanced directionality like the three other structures.

To further elucidate the role of the 2D array on directionality enhancement and also on resonant characteristics of the structures, the LHP of Structure 3 is eliminated altogether and the uniform random array residing on the RHP is analyzed (representative array shown as Structure 5 in the inset of Fig. 5(b)). Resonant wavelength and Q-factor of the most strongly confined modes obtained for different spatial configurations of Structure 5 are shown in Figs. 5(b)-(c) and the corresponding fraction of power emitted through the RHP is plotted in Fig. 5(d). As expected, directionality profiles of such arrays remain entirely random and no preferential direction of light transmission is observed. However, as can be observed from Fig. 5(b), localization wavelengths of these arrays reside well within the range of resonant wavelengths obtained for the composite systems of Structure 3. This confirms that localization wavelength of Structure 3 is primarily governed by multiple-scattering mediated strong-localization of light in its disordered portion of the overall structure. It is noteworthy that in spite of similar resonant wavelengths, Q-factors obtained for Structure 5 are about 2 to 3 orders of magnitude smaller than the values obtained with Structure 3. This is because light localization characteristics in Structure 5 are greatly diminished by the reduced size of the array. This is also indicative of the fact that the 2D periodic array

Optics EXPRESS

of Structure 3 plays an important role not only in attaining nearly unidirectional transmission characteristics, but also towards enhancing scattering mediated strong localization of light in the disordered medium.

It is to be noted that even though the present study utilizes 2D simulations, the design and findings of the work are applicable for practical three-dimensional (3D) structures as well where the nanowires will have finite heights. This has been confirmed by previous experimental studies, which showed that results obtained from 2D simulations are consistent with experimental results obtained from strong-localization of light in random arrays of nanowires [18,19] . As has been shown in recent reports on Anderson localization of light in nanowires, in 3D systems the nanowires guide the modes along the z-direction just like waveguides, and these modes are ultimately influenced at the tip of the nanowires by the air layer above the array [30,39]. Random-scattering mediated localization of light is still achieved in such 3D systems, though the resonant mode has a reduced Q-factor compared to its 2D counterpart. To have an estimate of the directionality profile of the 3D structures, 3D simulation of one of the arrays reported for Structure 3 has been performed in this work. In this simulation the nanowires are considered to be of 400 nm height and a gaussian pulse source has been placed in the center of the array at $z = 0$ plane (shown in Fig. 6(a)). The far- and near-field characteristics of the most strongly localized mode (at ~ 408 nm) obtained at this plane are shown in Figs. 6(b)-(c). These results confirm both light-localization and directionality enhancement along the RHP. To reduce mode-leakage from such 3D systems, InAlN or AlGaN-based cladding layers maybe introduced, which has been a standard practice in the design of III-nitride nanowire edge-emitting lasers [22,23]. It is also noteworthy that in experimental works involving 2D materials and optofluidic systems, strong-localization of light has been demonstrated based on 2D scattering medium as well [40–42].

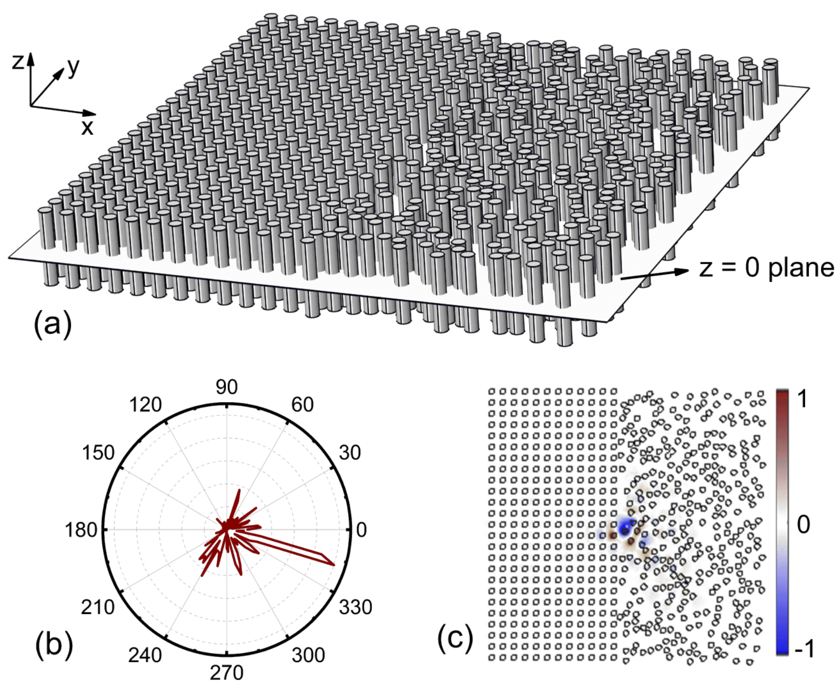

Fig. 6. (a) Schematic illustration of Structure 3 for which 3D simulation has been performed; (b) far-field directionality profile and (c) near-field image of the most strongly localized mode obtained for this 3D structure at $z = 0$ plane.

Optics EXPRESS

Hence in addition to the case of the 3D nanowire arrays, the proposed scheme of directionality enhancement is applicable to such 2D scattering medium based random arrays as well.

6. Conclusion

To summarize the key findings of this work, based on finite-difference time domain based numerical simulation and statistical analysis, it has been shown that in-plane directionality of a uniform random array of dielectric scatterers can be conveniently tuned by placing an appropriately designed 2D periodic or quasi-periodic array of scatterers adjacent to the 2D disordered medium. Such directionality enhancement is found to be related to the multiple-scattering governed wave dynamics of light in the periodic and random arrangements of the scatterers. Neither directionality enhancement, nor strong-localization is achieved when a one-dimensional periodic array in the form of a DBR is placed adjacent to the disordered array. This further confirms that in-plane 2D scattering plays the governing role in defining strong-localization and directionality of the proposed structures. Based on this principle, directionality profile of edge-emitting random lasers can be conveniently controlled by juxtaposing a 2D periodic or quasi-periodic array of scatterers next to self-organized nanowire arrays. While uniaxial random arrays similar to Structure 1 and 2 can be experimentally realized using modern lithography techniques like nanoimprint [43,44] or electron-beam lithography (EBL) [45], self-organized nanowire growth offers a convenient means of realizing uniform random arrays, like the ones appearing in Structure 3. Another approach would be to employ selective-area growth [46] and self-organized growth on the same substrate during MBE or MOCVD based epitaxy. In fact, this approach would enable experimental realization of half-periodic and half-uniform random arrays of nanowires (similar to Structure 3) during a single growth run. In addition to the discussions and analysis presented herein, there are numerous other aspects to look into related to the designs and concepts presented in this work. Aspects related to lasing have not been considered in this work as the present study aims to offer a generalized mechanism of directionality control in any random array of dielectric scatterers, which may or may not constitute in itself an active lasing medium. In lasing systems, the nanowires will contain active gain medium in the form of bulk, quantum-well, or quantum-dots, which will invariably emit and absorb light and therefore influence the lasing characteristics. While analysing random systems comprising active gain medium, these effects need to be taken into account to control in-plane directionality based on the proposed structures. In addition to these, there can be detailed investigation on the correlation between relative position of the source and location of the resonant mode in the arrays, and also on the size-dependence of periodic and random regions of the arrays in the context of directionality control. It will be also interesting to examine how the directionality and resonant characteristics of the disordered region will be influenced by a photonic crystal cavity introduced in the periodic region of the structure. Therefore, without any loss of generality, the proposed techniques of directionality enhancement in disordered systems offer the prospect of designing and realizing not only directionality tunable random lasers, but also disordered system based sensors, waveguides, couplers and numerous other photonic structures and systems with enhanced control and tunability.

Acknowledgments. The authors acknowledge the support and facilities obtained from the Department of Electrical and Electronic Engineering (EEE), Bangladesh University of Engineering and Technology (BUET).

Disclosures. The authors declare no conflicts of interest related to this article.

Data availability. Data underlying the results presented in this paper are not publicly available at this time but may be obtained from the authors upon reasonable request.

Supplemental document. See Supplement 1 for supporting content.

References

1. D. S. Wiersma, "Disordered photonics," Nat. Photonics **7**(3), 188–196 (2013).

2. S. Yu, C.-W. Qiu, Y. Chong, S. Torquato, and N. Park, "Engineered disorder in photonics," Nat. Rev. Mater. **6**(3), 226–243 (2021).
3. J. Liu, P. D. Garcia, S. Ek, N. Gregersen, T. Suhr, M. Schubert, J. Mørk, S. Stobbe, and P. Lodahl, "Random nanolasing in the Anderson localized regime," Nat. Nanotechnol. **9**(4), 285–289 (2014).
4. D. S. Wiersma, "The physics and applications of random lasers," Nat. Phys. **4**(5), 359–367 (2008).
5. Q. Song, S. Xiao, Z. Xu, J. Liu, X. Sun, V. Drachev, V. M. Shalaev, O. Akkus, and Y. L. Kim, "Random lasing in bone tissue," Opt. Lett. **35**(9), 1425–1427 (2010).
6. K. Vynck, M. Burresi, F. Riboli, and D. S. Wiersma, "Photon management in two-dimensional disordered media," Nat. Mater. **11**(12), 1017–1022 (2012).
7. J. Murray and J. N. Munday, "Experimental demonstration and modeling of the internal light scattering profile within solar cells due to random dielectric scatterers," J. Appl. Phys. **119**(2), 023104 (2016).
8. A. P. Mosk, A. Lagendijk, G. Lerosey, and M. Fink, "Controlling waves in space and time for imaging and focusing in complex media," Nat. Photonics **6**(5), 283–292 (2012).
9. J. Bertolotti, E. G. v. Putten, C. Blum, A. Lagendijk, W. L. Vos, and A. P. Mosk, "Non-invasive imaging through opaque scattering layers," Nature **491**(7423), 232–234 (2012).
10. S. H. Choi and Y. L. Kim, "The potential of naturally occurring lasing for biological and chemical sensors," Biomed. Eng. Lett. **4**(3), 201–212 (2014).
11. M. Gaio, S. Caixeiro, B. Marelli, F. G. Omenetto, and R. Sapienza, "Gain-Based Mechanism for pH Sensing Based on Random Lasing," Phys. Rev. Appl. **7**(3), 034005 (2017).
12. X. Wu, W. Fang, A. Yamilov, A. A. Chabanov, A. A. Asatryan, L. C. Botten, and H. Cao, "Random lasing in weakly scattering systems," Phys. Rev. A **74**(5), 053812 (2006).
13. Q. Song, L. Liu, S. Xiao, X. Zhou, W. Wang, and L. Xu, "Unidirectional High Intensity Narrow-Linewidth Lasing from a Planar Random Microcavity Laser," Phys. Rev. Lett. **96**(3), 033902 (2006).
14. T. Hisch, M. Liertzer, D. Pogany, F. Mintert, and S. Rotter, "Pump-Controlled Directional Light Emission from Random Lasers," Phys. Rev. Lett. **111**(2), 023902 (2013).
15. F. Tommasi, E. Ignesti, L. Fini, and S. Cavalieri, "Controlling directionality and the statistical regime of the random laser emission," Phys. Rev. A **91**(3), 033820 (2015).
16. S. Schönhuber, M. Brandstetter, T. Hisch, C. Deutsch, M. Krall, H. Detz, A. M. Andrews, G. Strasser, S. Rotter, and K. Unterrainer, "Random lasers for broadband directional emission," Optica **3**(10), 1035 (2016).
17. B. Abaie, E. Mobini, S. Karbasi, T. Hawkins, J. Ballato, and A. Mafi, "Random lasing in an Anderson localizing optical fiber," Light: Sci. Appl. **6**(8), e17041 (2017).
18. M. Sakai, Y. Inose, K. Ema, T. Ohtsuki, H. Sekiguchi, A. Kikuchi, and K. Kishino, "Random laser action in GaN nanocolumns," Appl. Phys. Lett. **97**(15), 151109 (2010).
19. K. H. Li, X. Liu, Q. Wang, S. Zhao, and Z. Mi, "Ultralow-threshold electrically injected AlGaN nanowire ultraviolet lasers on Si operating at low temperature," Nat. Nanotechnol. **10**(2), 140–144 (2015).
20. S. F. Yu, C. Yuen, S. P. Lau, W. I. Park, and G.-C. Yi, "Random laser action in ZnO nanorod arrays embedded in ZnO epilayers," Appl. Phys. Lett. **84**(17), 3241–3243 (2004).
21. A. Ghobadi, S. A. Dereshgi, H. Hajian, G. Birant, B. Butun, A. Bek, and E. Ozbay, "97 percent light absorption in an ultrabroadband frequency range utilizing an ultrathin metal layer: randomly oriented, densely packed dielectric nanowires as an excellent light trapping scaffold," Nanoscale **9**(43), 16652–16660 (2017).
22. P. Bhattacharya, A. Hazari, S. Jahangir, W. Guo, and T. Frost, "Chapter Eleven III-Nitride Electrically Pumped Visible and Near-Infrared Nanowire Lasers on (001) Silicon," Semicond. Semimetals **96**, 385–409 (2017).
23. A. Hazari, F. C. Hsiao, L. Yan, J. Heo, J. M. Millunchick, J. M. Dallesasse, and P. Bhattacharya, "Optical Interconnect on Silicon: A Monolithic III-Nitride Nanowire Photonic Integrated Circuit," IEEE J. Quantum Electron. **53**(4), 1–9 (2017).
24. D. J. Paul, A. A. Mimi, A. Hazari, P. Bhattacharya, and M. Z. Baten, "Finite-difference time-domain analysis of the tunability of Anderson localization of light in self-organized GaN nanowire arrays," J. Appl. Phys. **125**(4), 043104 (2019).
25. A. Lagendijk, B. Van Tiggelen, and D. S. Wiersma, "Fifty years of anderson localization," Phys. Today **62**(8), 24–29 (2009).
26. M. Segev, Y. Silberberg, and D. N. Christodoulides, "Anderson localization of light," Nat. Photonics **7**(3), 197–204 (2013).
27. T. Schwartz, G. Bartal, S. Fishman, and M. Segev, "Transport and anderson localization in disordered two-dimensional photonic lattices," Nature **446**(7131), 52–55 (2007).
28. B. Fazio, P. Artoni, M. A. Iatì, C. D'andrea, M. J. L. Faro, S. Del Sorbo, S. Pirotta, P. G. Gucciardi, P. Musumeci, C. S. Vasi, R. Saija, M. Galli, F. Priolo, and A. Irrera, "Strongly enhanced light trapping in a two-dimensional silicon nanowire random fractal array," Light: Sci. Appl. **5**(4), e16062 (2016).
29. T. Crane, O. J. Trojak, J. P. Vasco, S. Hughes, and L. Sapienza, "Anderson localization of visible light on a nanophotonic chip," ACS Photonics **4**(9), 2274–2280 (2017).
30. M. Rashidi, H. H. Tan, and S. Mokkapati, "Stable, multi-mode lasing in the strong localization regime from inp random nanowire arrays at low temperature," Optica **8**(9), 1160–1166 (2021).
31. T. Frost, S. Jahangir, E. Stark, S. Deshpande, A. Hazari, C. Zhao, B. S. Ooi, and P. Bhattacharya, "Monolithic Electrically Injected Nanowire Array Edge-Emitting Laser on (001) Silicon," Nano Lett. **14**(8), 4535–4541 (2014).

32. A. Hazari, A. Aiello, T.-K. Ng, B. S. Ooi, and P. Bhattacharya, "III-nitride disk-in-nanowire 1.2 μm monolithic diode laser on (001)silicon," Appl. Phys. Lett. **107**(19), 191107 (2015).
33. N. Wang, Y. Cai, and R. Zhang, "Growth of nanowires," Mater. Sci. Eng. R: Reports **60**(1-6), 1–51 (2008).
34. A. F. Oskooi, D. Roundy, M. Ibanescu, P. Bermel, J. Joannopoulos, and S. G. Johnson, "Meep: A flexible free-software package for electromagnetic simulations by the FDTD method," Comput. Phys. Commun. **181**(3), 687–702 (2010).
35. V. A. Mandelshtam and H. S. Taylor, "Harmonic inversion of time signals and its applications," The J. Chem. Phys. **107**(17), 6756–6769 (1997).
36. M. I. Tahmid, D. J. Paul, and M. Z. Baten, "Emergence and tunability of transmission gap in the strongly disordered regime of a dielectric random scattering medium," Opt. Express **29**(11), 17215 (2021).
37. D. J. Paul, S. Hossain, and M. Z. Baten, "Disorder induced rotational-symmetry breaking to control directionality of whispering gallery modes in circularly symmetric nanowire assembly," Opt. Express **27**(16), 23645 (2019).
38. A. K. Boddeti, R. Kumar, and S. Mujumdar, "Figures-of-merit of anderson localization cavities in membrane-based periodic-on-average random templates," Opt. Commun. **397**, 39–43 (2017).
39. M. Rashidi, Z. Li, C. Jagadish, S. Mokkapati, and H. H. Tan, "Controlling the lasing modes in random lasers operating in the anderson localization regime," Opt. Express **29**(21), 33548–33557 (2021).
40. P. I. Pincheira, M. L. da Silva Neto, M. Maldonado, C. B. de Araújo, A. M. Jawaid, R. Busch, A. J. Ritter, R. A. Vaia, and A. S. Gomes, "Monolayer 2d zrte 2 transition metal dichalcogenide as nanoscatter for random laser action," Nanoscale **12**(29), 15706–15710 (2020).
41. A. Sarkar and B. S. Bhaktha, "Signatures of periodicity and randomness in the angular emission profile of a 2-d on-average periodic optofluidic random laser," Opt. Lett. **40**(21), 4951–4954 (2015).
42. T. Dixit, A. Arora, A. Krishnan, K. L. Ganapathi, P. K. Nayak, and M. R. Rao, "Near infrared random lasing in multilayer mos2," ACS Omega **3**(10), 14097–14102 (2018).
43. A. A. Talin, L. L. Hunter, F. Léonard, and B. Rokad, "Large area, dense silicon nanowire array chemical sensors," Appl. Phys. Lett. **89**(15), 153102 (2006).
44. A. Zhang, H. Kim, J. Cheng, and Y.-H. Lo, "Ultrahigh Responsivity Visible and Infrared Detection Using Silicon Nanowire Phototransistors," Nano Lett. **10**(6), 2117–2120 (2010).
45. Z. Li, Y. Chen, X. Li, T. I. Kamins, K. Nauka, and R. S. Williams, "Sequence-Specific Label-Free DNA Sensors Based on Silicon Nanowires," Nano Lett. **4**(2), 245–247 (2004).
46. A. Roshko, M. Brubaker, P. Blanchard, T. Harvey, and K. A. Bertness, "Selective Area Growth and Structural Characterization of GaN Nanostructures on Si(111) Substrates," Crystals **8**(9), 366 (2018).